

# The Antarctic Ozone Hole during 2013

Andrew R. Klekociuk<sup>1,2</sup>, Paul B. Krummel<sup>3</sup>, Matthew B. Tully<sup>4</sup>, H. Peter Gies<sup>5</sup>,  
Simon P. Alexander<sup>1,2</sup>, Paul J. Fraser<sup>3</sup>, Stuart I. Henderson<sup>5</sup>, John  
Javorniczky<sup>5</sup>, Jonathon D. Shanklin<sup>6</sup>, Robyn Schofield<sup>7,8</sup> and Kane A. Stone<sup>7,8</sup>

<sup>1</sup> Antarctica and the Global System, Australian Antarctic Division, Hobart, Australia

<sup>2</sup> Antarctic Climate and Ecosystems Cooperative Research Centre, Hobart, Australia

<sup>3</sup> CSIRO Oceans and Atmosphere Flagship, Melbourne, Australia

<sup>4</sup> Bureau of Meteorology, Melbourne, Australia

<sup>5</sup> Australian Radiation Protection and Nuclear Safety Agency, Melbourne, Australia

<sup>6</sup> British Antarctic Survey, Cambridge, United Kingdom

<sup>7</sup> School of Earth Sciences, University of Melbourne, Melbourne, Australia

<sup>8</sup> ARC Centre of Excellence for Climate System Science, University of New South Wales, Sydney, Australia

(Manuscript received March 2015; accepted November 2015)

We review the 2013 Antarctic ozone hole, making use of various ground-based, *in-situ* and remotely-sensed ozone measurements, ground-based measurements of ultraviolet radiation and meteorological reanalyses. Based on analysis of 34 years of satellite records spanning 1979–2013 (which excludes 1995), we find that in terms of maximum area, minimum ozone level and total ozone deficit, the ozone hole in 2013 was typical of other years of moderate ozone loss. The estimated integrated ozone mass effectively depleted within the ozone hole of 2013 was approximately 1037 Mt, which was the 17<sup>th</sup> largest deficit on record and 41% of the peak deficit observed in 2006. Anomalously cold winter temperatures in the lower stratosphere over Antarctica and concurrent strong and stable vortex conditions favoured the potential for strong ozone depletion in 2013. However, anomalous warming of the polar vortex that occurred from late August limited the overall severity of ozone depletion during spring, and resulted in the relatively early breakup of the ozone hole in mid-November.

## Introduction

An ozone hole continues to form over Antarctica each austral spring due to the combined action of man-made ozone depleting substances (ODS) and the special meteorological conditions that occur during the polar night (Tully et al., 2008; Dameris and Godin-Beekmann, 2014). In mid- to late autumn (April–May), a vortex forms in the lower stratosphere over Antarctica effectively isolating the enclosed air mass from mixing with the rest of the atmosphere. Within the vortex, air radiatively cools to the point where Polar Stratospheric Cloud (PSC) particles can exist. During winter, reservoir halogen compounds originating from ODS are converted into active species by reactions on the surfaces of PSC particles and other stratospheric aerosols. From late winter (August), ozone levels in the lower stratosphere begin to decline as the active halogenated species are photolysed by sunlight, thereby releasing chlorine and bromine atoms that destroy ozone in a catalytic cycle. By mid-September, when the peak of ozone depletion takes place, average total column ozone levels over much of Antarctica are reduced by more than 50%. From late spring (November) to early summer (December), the ozone hole breaks down as warming of the atmosphere evaporates PSCs and the polar vortex disperses.

International controls on the emission of ODS are leading to a reduction in levels of man-made chlorine and bromine compounds in the troposphere (Klekociuk et al., 2014). In 2013, the estimated level of Equivalent Effective Stratospheric Chlorine (EESC) over Antarctica, which is a measure of the ozone depleting potential of ODS reaching the stratosphere, was approximately 91% of the peak value in 2000 (Klekociuk et al., 2014, Figure 8). On this basis, ozone recovery in the years since 2000 can be expected to have been relatively modest compared with the EESC change of approximately 50%

that is estimated to have taken place between 1979 (the year for which the first unambiguous ozone hole was identified in the satellite record) and 2000. While there is some suggestion in a reversal of Antarctic ozone levels after 2000 (e.g. Klekociuk et al., 2014b, Figure 4), it is evident that meteorological processes have a significant impact on inter-annual variability in ozone hole metrics. For example, years of anomalously reduced ozone depletion compared with the expectation based solely on regressions against EESC were observed in 1988, 2002, 2004, 2010 and 2012; during these years, the polar vortex was anomalously disturbed, which was a key factor in inhibiting ozone depletion (Klekociuk et al., 2011, 2014b).

Here we present an analysis of the Antarctic ozone hole in 2013, continuing a series of earlier papers (Tully et al., 2008, 2011; Klekociuk et al., 2011, 2014a,b) that assess the characteristics and circumstances of ozone holes in specific years in relation to prevailing meteorological conditions and ODS levels. We use a range of Australian data and analyses including analyses of satellite measurements by the Commonwealth Scientific and Industrial Research Organisation (CSIRO) Oceans and Atmosphere Flagship, ozone measurements obtained by the Australian Antarctic Division (AAD) and the Bureau of Meteorology (BoM), and Antarctic ultraviolet radiation measurements from the Australian Radiation Protection and Nuclear Safety Agency (ARPANSA) biometer network. Other data from satellite and ground-based instruments and meteorological reanalyses are also presented. This work complements other analyses of Antarctic atmospheric conditions and ozone depletion during 2013 provided by the World Meteorological Organisation (WMO) Antarctic Ozone Bulletins (URL <http://www.wmo.int/pages/prog/arep/gaw/ozone/index.html>), upper-air summaries of the National Climate Data Center (NCDC; URL <http://www.ncdc.noaa.gov/sotc/upper-air>) and by Blunden and Arndt (2014; URL <http://www.ncdc.noaa.gov/bams-state-of-the-climate>).

## Total column ozone measurements

### Ozone hole metric summary and rankings

As in previous papers in this series, we evaluate specific metrics for the ozone hole using total column ozone measurements from the Total Ozone Mapping Spectrometer (TOMS) series of satellite instruments and the Ozone Monitoring Instrument (OMI) on the Aura satellite that have been processed with the TOMS version 8.5 algorithm (see Klekociuk et al. (2014b) for details). Table 1 contains the ranking for all 34 ozone holes analysed since 1979 using 8 metrics that measure the 'size' of the Antarctic ozone hole (see the notes accompanying the Table for the definition of each metric and the datasets and years considered). The first 7 metrics in Table 1 measure various aspects of the area and depth of the ozone hole and the 2013 ozone hole was ranked between 17<sup>th</sup> and 22<sup>nd</sup> in terms of severity across these metrics. Figure 1a shows the daily ozone hole area throughout the 2013 season. The annual maximum value of the daily area (metric 2) is often used to describe the overall size of the ozone hole; in 2013 this metric was the 17<sup>th</sup> largest on record, attaining 24.0 million km<sup>2</sup> in mid-September (compared with surface areas of Antarctica and Australia of 14 Mkm<sup>2</sup> and 7.7 Mkm<sup>2</sup>, respectively). While the ranking is mid-range (17 out of 34), this was one of the smallest values observed for this metric over most years since 1992, with the exception of 2002, 2004, 2010 and 2012 (noting that ozone depletion was enhanced in 1992 and 1993 from the effects of Mt. Pinatubo (Knight et al., 1998)).

It is evident from Figure 1a that the growth of the ozone hole in 2013 was similar to or slightly greater than the climatological mean, and generally more rapid than in 2010 and 2012. The area of the ozone hole peaked around mid-September, and this was followed by a general decline that was relatively rapid after October 10. Of particular note is that the area metric showed a similarly rapid decline to that observed in 2012, and a breakdown date (area first less than 0.5 Mkm<sup>2</sup>) of 16 November that was earlier than all measured years since 1988 with the exception of 2002 and 2012.

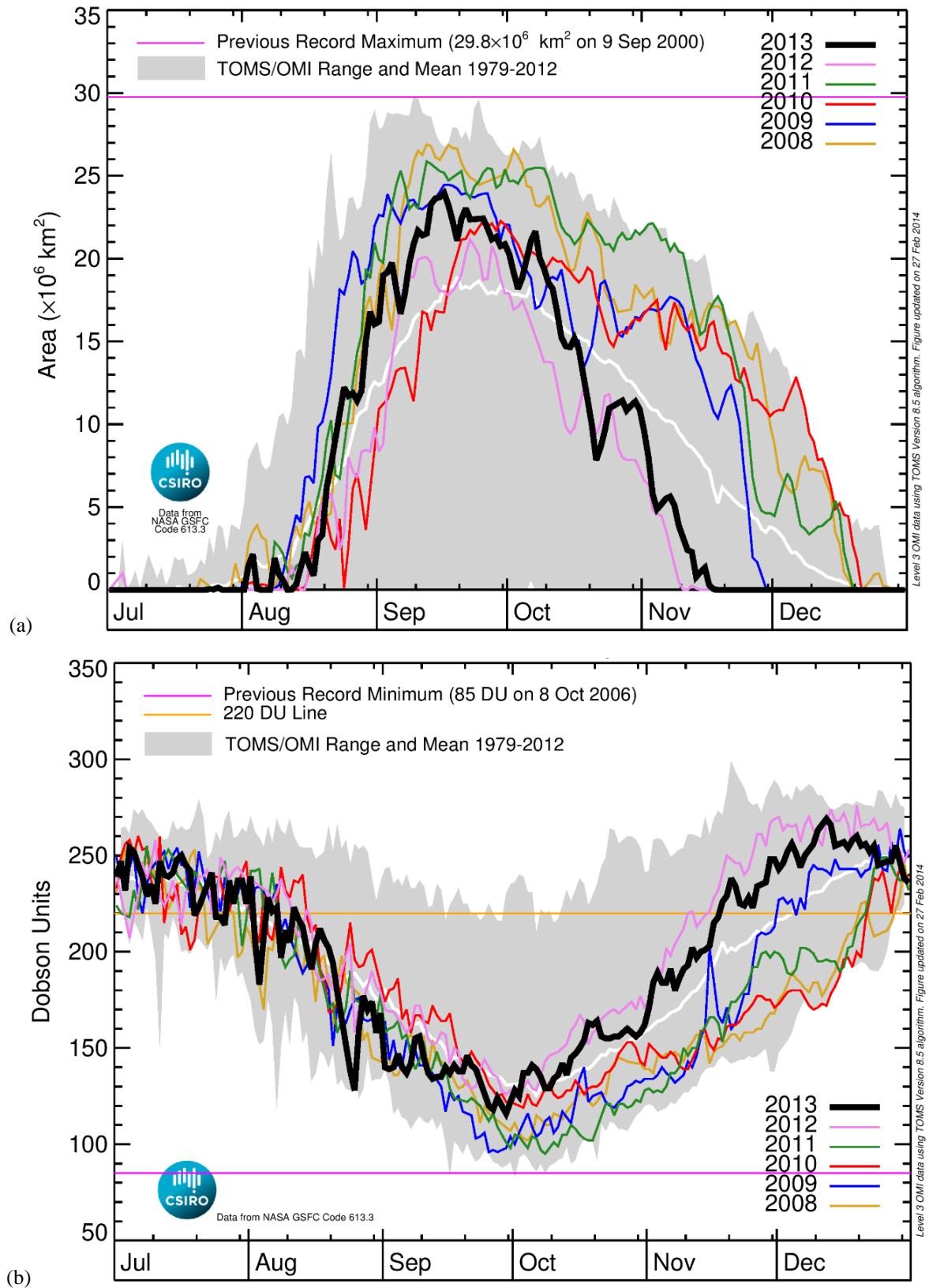
As shown in Figure 1b, the progression of the daily minimum total column ozone amount up to the end of September in 2013 was generally at or below the 1979-2012 climatological mean. From about August 20<sup>th</sup>, the minimum ozone value rapidly declined to reach a value of 128 DU on the 25<sup>th</sup> and then rebounded towards the climatological mean over the following few days. This period was associated with the development of a pronounced asymmetry in the shape of the ozone hole due to the development of a strong quasi-stationary wave-1 planetary wave outside of the vortex (not shown). At this time, the edge of the vortex out to approximately 60°S in the Pacific region west of South America was exposed to sunlight (not shown) which potentially enhanced ozone destruction in that sector of the vortex. Similar to the behaviour in 2012, minimum observed total column values from October until mid-December were mostly above the climatological mean, which contrasted with the behaviour during the other years shown for which ozone levels were generally below the mean.

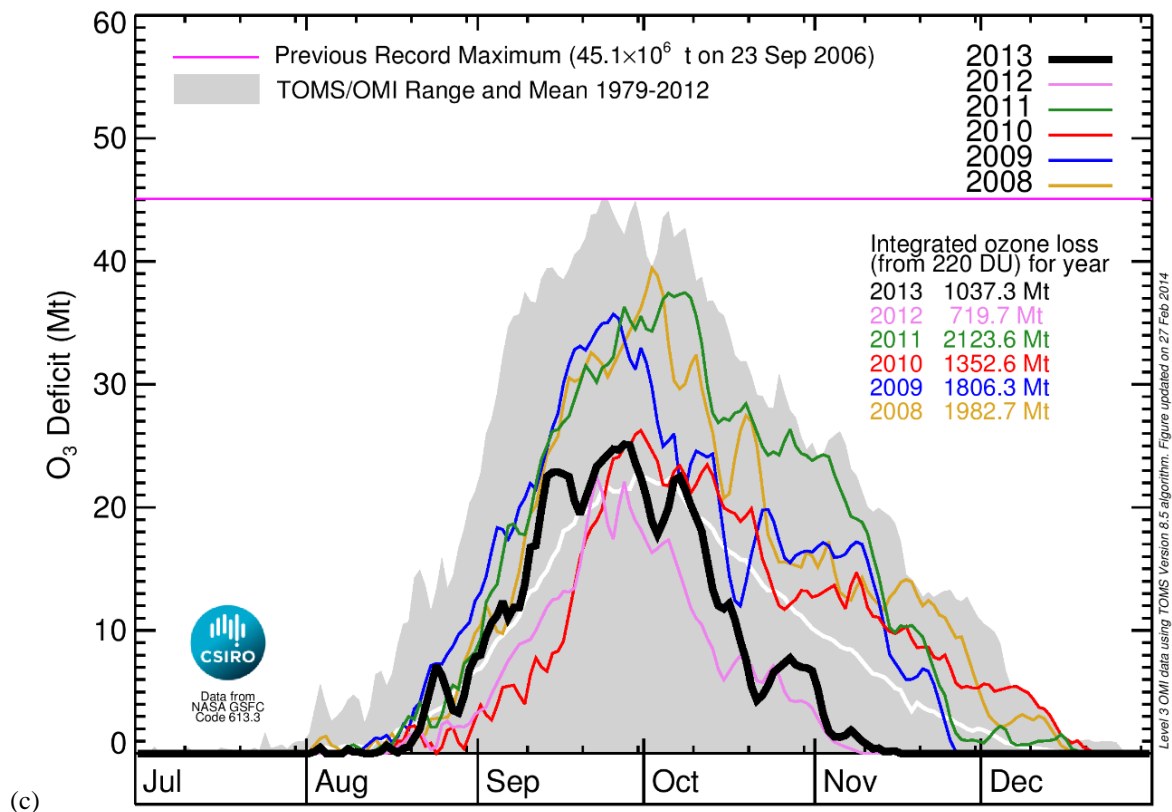
**Table 1** Ranked Antarctic ozone hole metrics obtained from TOMS/OMI satellite data. The 2005 metrics are the average of TOMS and OMI data; TOMS data are used exclusively before 2005 and OMI data are used exclusively after 2005. Rank 1 = lowest ozone minimum, greatest area, greatest ozone loss etc.; Rank 2 = second lowest ozone minimum, etc. There was a gap in TOMS coverage during the growth of the 1994 ozone hole; metrics for some parameters for that year are therefore undetermined and are left blank. There were no relevant TOMS measurements in 1995. Metric Definitions: 1. Maximum 15-day averaged area: The largest value (in each year) of the daily ozone hole area averaged using a 15-day sliding time interval. 2. Daily maximum area: The maximum daily value of the ozone hole area. 3. Minimum 15-day averaged total column ozone: The minimum of the 15-day averaged column ozone amount observed south of 35 °S. 4. Daily minimum total column ozone: The minimum of the daily column ozone amount observed south of 35 °S. This metric effectively measures the ‘depth’ of the ozone hole. 5. Daily minimum average total column ozone: The minimum of the daily column ozone amount averaged within the ozone hole. This metric effectively measures the ‘average depth’ of the ozone hole. 6. Maximum daily ozone deficit: The maximum value of the daily total ozone deficit within the ozone hole. This metric effectively measures the combined area and depth of the ozone hole. 7. Integrated ozone deficit: The integrated (total) daily ozone deficit for the entire ozone hole season. This metric effectively measures the overall severity of ozone depletion. 8. Breakdown date: The final date at which the daily maximum area (metric 2) falls below 0.5 million km<sup>2</sup>. Note that the metrics use 220 DU as the threshold in total column ozone to define the location and occurrence of the ozone hole.

Metric	1. Maximum 15-day averaged area		2. Daily maximum area		3. Minimum 15-day averaged total column ozone		4. Daily minimum total column ozone		5. Daily minimum average total column ozone		6. Daily maximum ozone deficit		7. Integrated ozone deficit		8. Breakdown Date	
	Rank	Year	10 <sup>6</sup> km <sup>2</sup>	Year	10 <sup>6</sup> km <sup>2</sup>	Year	DU	Year	DU	Year	DU	Year	Mt	Year	Mt	Year
1	2000	28.7	2000	29.8	2000	93.5	2006	85	2000	138.3	2006	45.1	2006	2560	1999	27-Dec (361)
2	2006	27.6	2006	29.6	2006	93.7	1998	86	2006	143.6	2000	44.9	1998	2420	2008	26-Dec (361)
3	2003	26.9	2003	28.4	1998	96.8	2000	89	1998	146.7	2003	43.4	2001	2298	2010	21-Dec (355)
4	1998	26.8	1998	27.9	2001	98.9	2001	91	2003	147.5	1998	41.1	1999	2250	2001	19-Dec (353)
5	2008	26.1	2005	27.0	1999	99.9	2003	91	2005	148.8	2008	39.4	1996	2176	2011	19-Dec (353)
6	2001	25.7	2008	26.9	2011	100.9	2005	93	2001	148.8	2001	38.5	2000	2164	2006	16-Dec (350)
7	2005	25.5	1996	26.8	2003	101.9	1991	94	1999	149.3	2005	37.7	2011	2124	1990	15-Dec (349)
8	2011	25.1	2001	26.4	2005	102.8	2011	95	2009	150.4	2011	37.5	2008	1983	2007	15-Dec (349)
9	1996	25.0	2011	25.9	2009	103.1	2009	96	1996	150.6	2009	35.7	2005	1895	1998	13-Dec (347)
10	1993	24.8	1993	25.8	1993	104.0	1999	97	2008	150.8	1999	35.3	2003	1894	2005	11-Dec (345)

11	1994	24.3	1999	25.7	1996	106.0	1997	99	2011	151.2	1997	34.5	1993	1833	1992	08-Dec (343)
12	2007	24.1	1994	25.2	1997	107.2	2008	102	1997	151.3	1996	33.9	2009	1806	1996	08-Dec (343)
13	2009	24.0	2007	25.2	2008	108.9	2004	102	2007	155.1	1992	33.5	2007	1772	1987	08-Dec (342)
14	1992	24.0	1997	25.1	1992	111.5	1996	103	1993	155.2	2007	32.9	1997	1759	2004	05-Dec (340)
15	1999	24.0	1992	24.9	2007	112.7	1993	104	1992	156.3	1993	32.6	1992	1529	2003	05-Dec (339)
16	1997	23.3	2009	24.5	1991	113.4	1992	105	1991	162.5	1991	26.6	1987	1366	1993	04-Dec (338)
17	<b>2013</b>	<b>22.7</b>	<b>2013</b>	<b>24.0</b>	1987	115.7	1989	108	1987	162.6	2010	26.2	2010	1353	1985	03-Dec (337)
18	2010	21.6	2004	22.7	2004	116.0	2007	108	1990	164.4	1987	26.2	1990	1181	1997	03-Dec (337)
19	1987	21.4	1987	22.4	1990	117.8	1987	109	2010	164.5	<b>2013</b>	<b>25.1</b>	<b>2013</b>	<b>1037</b>	1989	01-Dec (335)
20	2004	21.1	1991	22.3	1989	120.4	1990	111	<b>2013</b>	<b>164.7</b>	1990	24.3	1991	998	1984	28-Nov (333)
21	1991	21.0	2010	22.3	2010	124.3	<b>2013</b>	<b>116</b>	1989	166.2	1989	23.6	2004	975	2009	29-Nov (333)
22	1989	20.7	2002	21.8	<b>2013</b>	<b>127.8</b>	2010	119	2004	166.7	2002	23.2	1989	917	1994	25-Nov (329)
23	1990	19.5	1989	21.6	1985	131.8	1985	124	2002	169.8	2004	22.8	2012	720	2000	19-Nov (324)
24	2012	19.3	2012	21.2	2012	131.9	2012	124	2012	170.2	2012	22.5	1985	630	1991	18-Nov (322)
25	2002	17.7	1990	21.0	2002	136.0	2002	131	1985	177.1	1985	14.5	2002	575	<b>2013</b>	<b>16-Nov (320)</b>
26	1985	16.6	1985	18.6	1986	150.3	1986	140	1986	184.7	1986	10.5	1986	346	1986	14-Nov (318)
27	1986	13.4	1984	14.4	1984	156.1	1984	144	1984	190.2	1984	9.2	1984	256	1982	12-Nov (316)
28	1984	13.0	1986	14.2	1983	160.3	1983	154	1983	192.3	1983	7.0	1988	198	2012	07-Nov (312)
29	1988	11.3	1988	13.5	1988	169.4	1988	162	1988	195.0	1988	6.0	1983	184	1980	06-Nov (311)
30	1983	10.1	1983	12.1	1982	183.3	1982	170	1982	199.7	1982	3.7	1982	73	2002	06-Nov (310)
31	1982	7.5	1982	10.6	1980	200.0	1980	192	1980	210.0	1980	0.6	1980	13	1983	05-Nov (309)
32	1980	2.0	1980	3.2	1981	204.0	1979	194	1979	210.2	1981	0.6	1981	4	1981	31-Oct (304)
33	1981	1.3	1981	2.9	1979	214.7	1981	195	1981	210.2	1979	0.3	1979	1	1988	26-Oct (300)
34	1979	0.2	1979	1.2	1994		1994		1994		1994		1994		1979	19-Sep (262)

Figure 1 Estimated daily (a) ozone hole area, (b) ozone hole depth and (b) ozone mass deficit based on OMI satellite data.





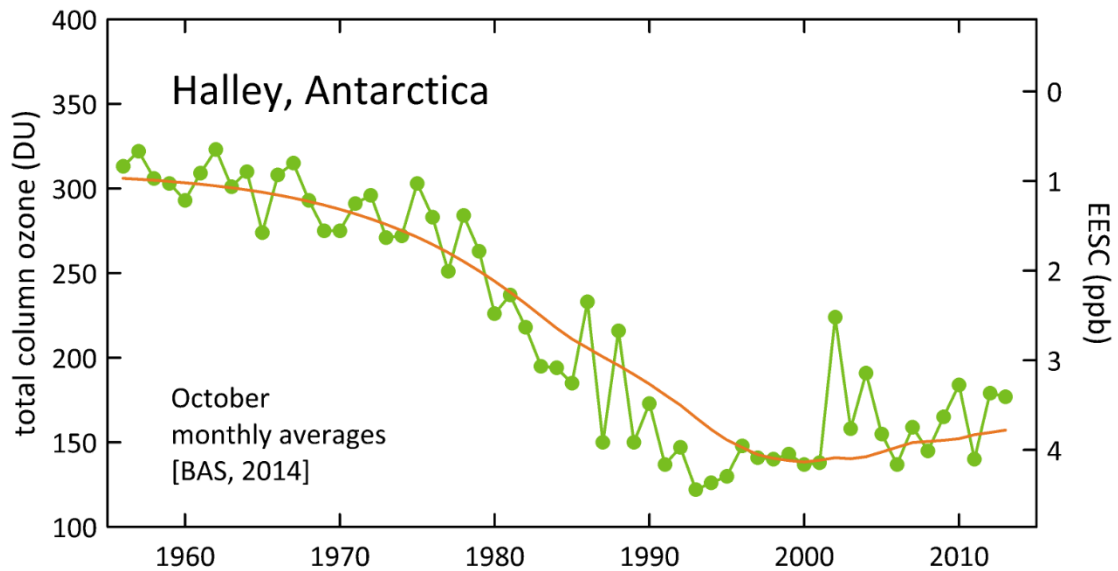
The overall minimum total column amount (metric 4) of 116 DU attained at the end of September was ranked the 21<sup>st</sup> lowest annual minimum observed. Figure 1c shows the daily ozone deficit, which measures the total mass of ozone effectively depleted within the area of the ozone hole. The maximum daily ozone deficit (metric 6) of 25.1 Mt was attained in early October, which was the 19<sup>th</sup> largest annual maximum observed. A metric which gauges the overall severity of the ozone hole is the total annual deficit (metric 7); at 1037 Mt, this was the 19<sup>th</sup> largest deficit on record and 41% of the peak value observed in 2006.

Figure 2 shows the timeseries of October monthly average total ozone column values from Halley, Antarctica. The observed value for 2013 was high in comparison to most years since 1990; larger values were observed only in 2002, 2004, 2010 and 2012 (largest to smallest). Indeed, if we consider the difference of the observations from the regression against EESC (not shown), 2013 had the 7<sup>th</sup> highest positive deviation of all years since 1956 (larger deviations (ordered largest to smallest) were observed in 2002, 2004, 2010, 1986, 2012 and 1988). While relatively high, the Halley October mean in 2013 was not significantly different (at the 95% confidence limit) to the minimum of the regression curve shown in Figure 2.

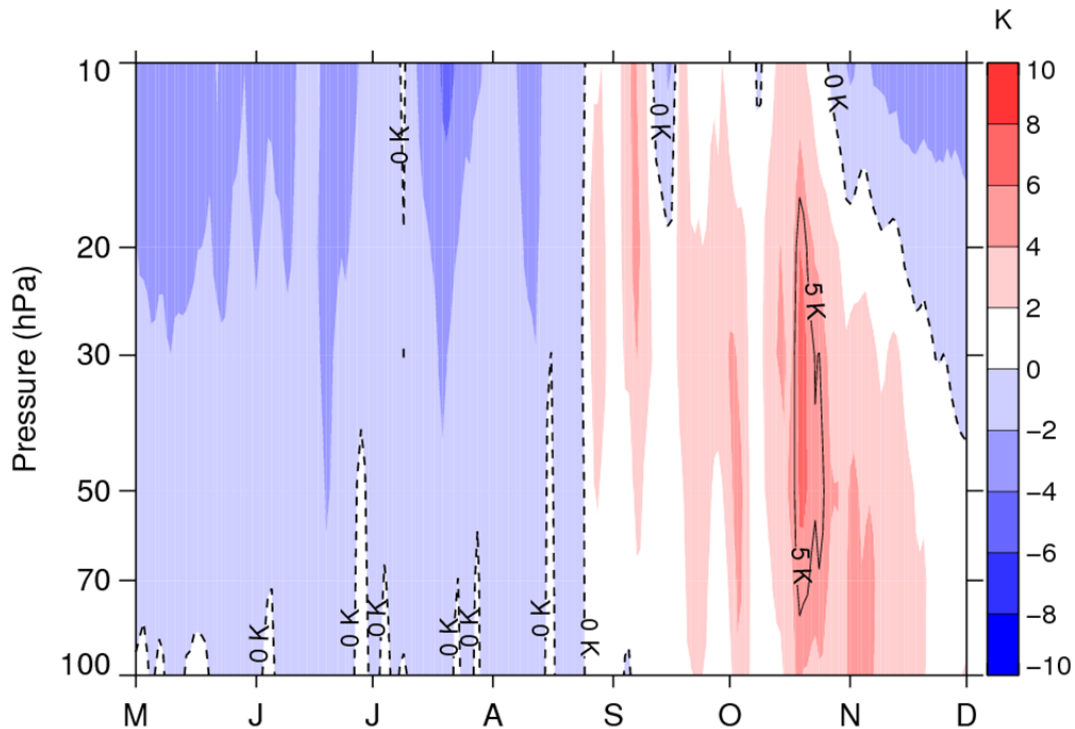
The behaviour of the metrics shown in Figures 1 and 2 is consistent with two distinct influences from meteorological factors during 2013. Firstly, the stratospheric polar vortex was relatively cold and stable during winter compared with the long-term climatological average. Figure 3 shows the pressure-time structure of the climatological zonal mean temperature anomaly for the latitude band 55°S - 75°S (which spans the latitude range of the vortex edge) obtained from the National Centers for Environment Prediction (NCEP) – Department of Energy (DOE) Reanalysis 2 meteorological data (Kanamitsu et al., 2002). Up to late August, anomalously cold temperatures are apparent, particularly in the upper levels, indicating that the vortex was relatively unaffected by the poleward transport of heat that normally accompanies mid-latitude planetary wave activity in winter. As suggested by Figure 3, polar cap (60°S-90°S) winter temperatures in the lower stratosphere were also below average (Appendix, Figures 8 and 9). For example, 50 hPa temperatures for July were 2 K below the average for 1979-2012, and ranked as the coldest for the preceding decade (Appendix, Figure 8). The cold temperatures would be expected to enhance the formation of PSCs during winter and thereby also enhance the formation of active ozone-depleting compounds. As described in the Appendix, other indicators of polar temperature as well as metrics of dynamical activity and the polar vortex in the lower stratosphere (Figures 8-11) suggest that during the 2013 winter, the polar

vortex was relatively stable and slightly above average size. Overall, the relatively rapid growth that occurred in the ozone hole area (Figure 1a) and mass deficit (Figure 1c) during August compared with other recent years is consistent with favourable preconditioning having taken place during winter within the polar vortex to promote ozone depletion once sunlight began returning to the polar cap.

Figure 2 October monthly mean total column ozone values for Halley station for 1957–2013 (green points and line) and regression to Equivalent Effective Stratospheric Chlorine (orange line) from Fraser et al. (2014) using a mean age of air of 5 years.



**Figure 3** Pressure-time cross section of the 2013 NCEP-DOE Reanalysis 2 zonal mean temperature anomaly in the lower stratosphere for the latitude range  $55^{\circ}\text{S} - 75^{\circ}\text{S}$  with respect to the 1979-2012 climatology. Red (blue) colours indicate temperatures warmer (cooler). The start of months May to December is indicated by the vertical ticks on the horizontal axis.



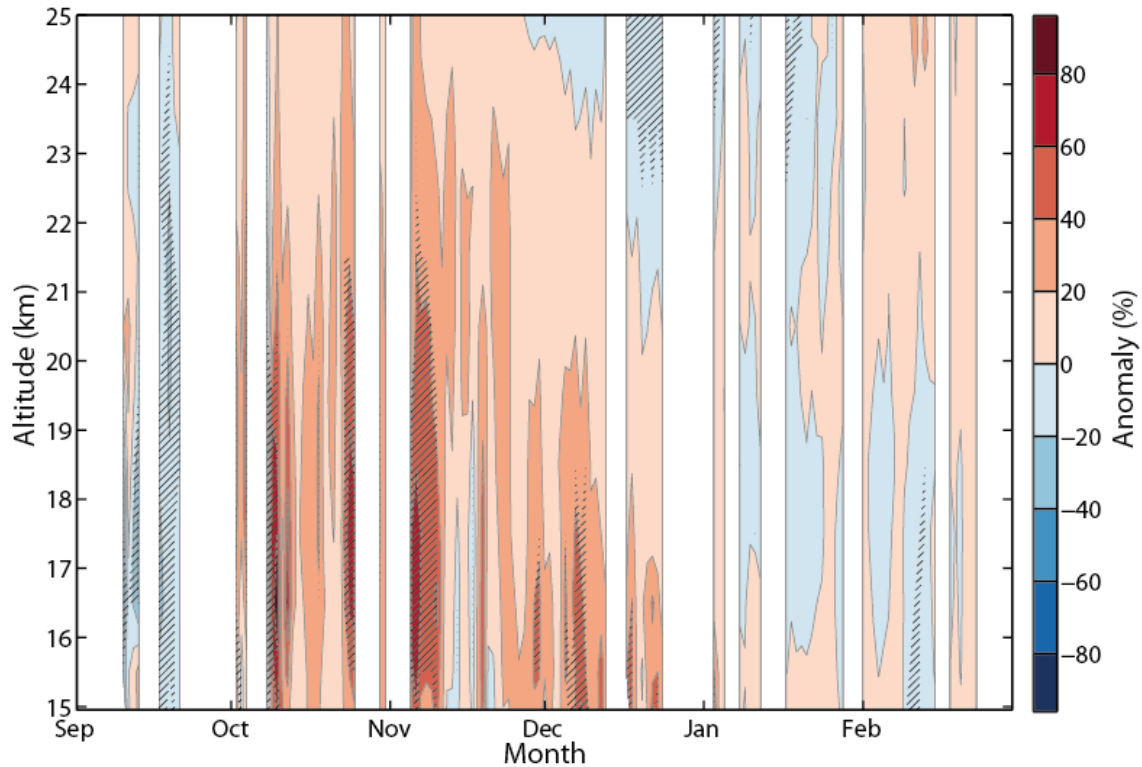
Secondly, from late August the stability of the vortex began to decline as the edge of the vortex warmed (Figure 3) and planetary wave activity outside the vortex promoted the transport of heat into the polar cap (Appendix, Figures 9 and 10b). The influence of the dynamical activity was most pronounced in the Antarctic lower stratosphere from mid-October (Figure 3 and Appendix, Figure 11a) when the area of the vortex began to rapidly decline. Overall, the level and persistence of dynamical activity during spring appears to have been an important factor in causing the ozone hole to breakdown relatively early (in mid-November) and in limiting the overall severity of Antarctic ozone loss during 2013.

## Vertically resolved ozone measurements

### Odin OSIRIS stratospheric ozone profiles

Figure 4 summarises the time-height development of the anomaly in ozone density over the southern polar cap (poleward of  $60^{\circ}\text{S}$ ) from September 2013 to February 2014. This figure uses vertical profiles of stratospheric ozone number density obtained from the Optical Spectrograph and Infra-Red Imager System (OSIRIS) instrument on-board the Odin satellite (see Klekociuk et al. (2014b) for details), and the anomaly (expressed as a percentage deviation) has been evaluated using the climatological mean over corresponding days between 2003 and 2013. Figure 4 indicates that during the few available days of measurement in September, polar cap ozone concentrations in the lower stratosphere (below 20 km) were below the climatological mean, while from October through December, ozone concentrations in this region were anomalously high (exceeding 50% above the mean at times).

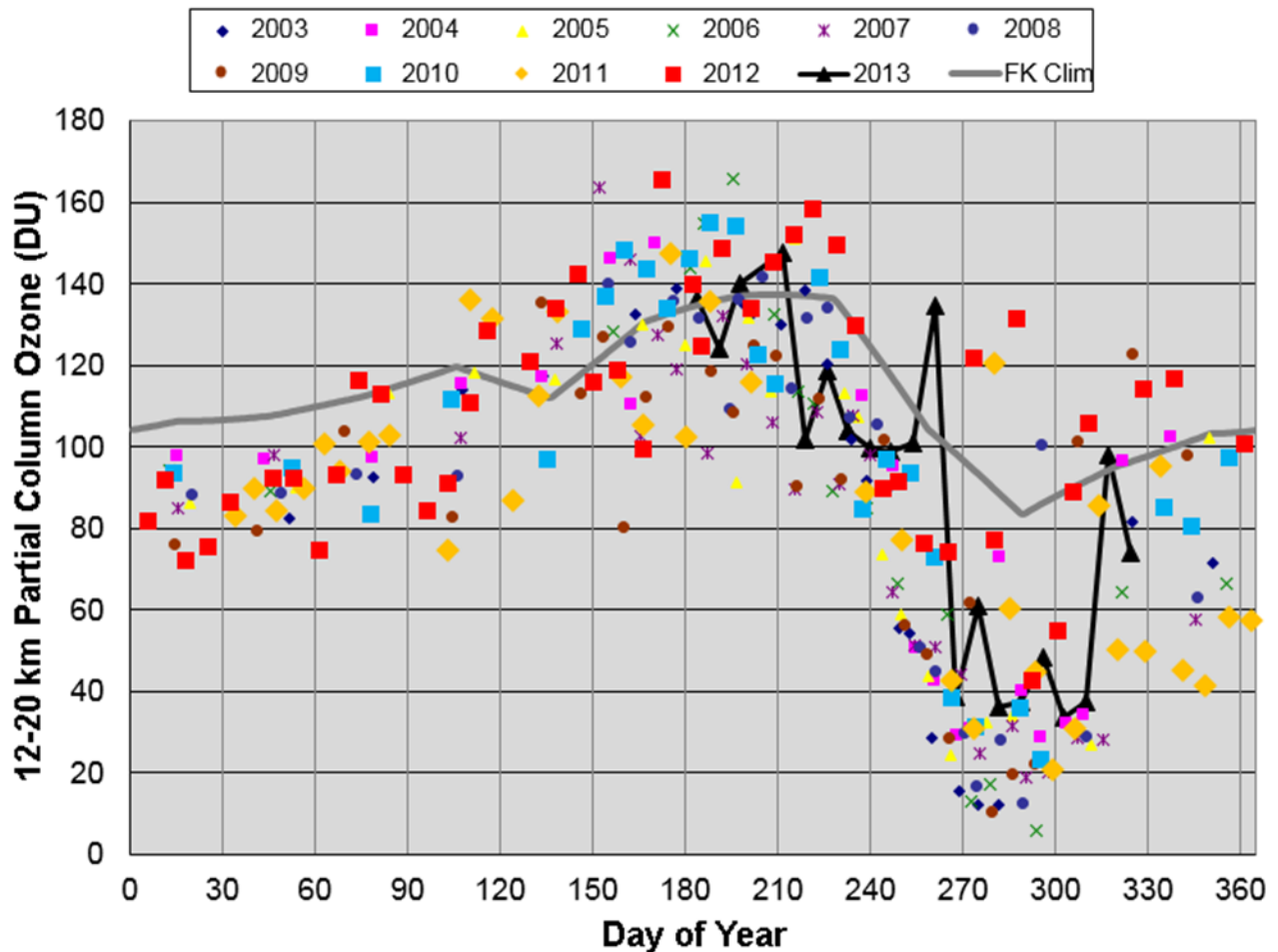
Figure 4 Time-height cross-section of OSIRIS daily zonal mean stratospheric ozone number density anomaly averaged over latitudes 60°S-83°S for September to February 2013-2014. The anomaly at each height is evaluated relative to the corresponding days for 2003-2013 climatological period. White gaps indicate time periods when no measurements were performed. Hatching is shown where the anomaly is above (below) the 90th (10th) percentiles over the climatological period.



### Ozonesonde measurements at Davis

In 2013, the program of ozonesonde profiling of the troposphere and lower stratosphere at Australia's Davis station in Antarctica (68.6°S, 78.0°E) continued. This involved balloon launches at approximately weekly intervals from July to November. Figure 5 shows the 12-20 km partial column ozone amount for 2013 in comparison with earlier measurements. Generally, the partial column concentrations between 28 September (day 268) and 5 November (day 310) were higher than most of the other measurements in this interval during 2003-2012. Notable high concentration values for the partial column were on 17 September (day 261) when the vortex was displaced off-pole towards South America and Davis was outside the vortex core (not shown), and 13 November (day 317) during the breakdown of the vortex (see Appendix).

Figure 5 Timeseries of partial column ozone for the height interval 12–20 km obtained from ozonesonde measurements at Davis, Antarctica (68.6°S, 78.0°E). Shown are data for all years of measurement, with data for 2013 highlighted in black. The grey line is the climatological mean for 1980–1991 from Fortuin and Kelder (1998) interpolated to the location of Davis.



## Antarctic ultraviolet radiation

Measurements of biologically effective solar ultraviolet radiation (UVR) continued in 2013 at Casey (66.3°S, 110.5°E), Mawson (67.6°S, 62.9°E) and Davis in Antarctica. Details on the instrumentation and methods used are provided by Tully et al. (2008) and Klekociuk et al. (2014b).

Figure 6 compares Ultraviolet (UV) Index measurement at Davis with total column ozone measurements for the site obtained from the OMI instrument (similar figures for Casey and Mawson are presented in the Appendix, Figure 12). The UV Index (WHO, 2002) is a measure of the intensity of solar UVR at Earth's surface taking into account its biological effects on human skin. There are two main aspects to the variability in the daily UV index values apparent in Figure 6. Firstly, there is a seasonal dependence due to variations in the minimum solar zenith angle (apparent height of the sun in the sky at solar noon). Secondly, local weather conditions (cloud cover) and varying stratospheric ozone exert a day-to-day influence on the measured solar UVR. For clear-sky days there is a strong anti-correlation between the measured UV Index and total column ozone, where low ozone results in higher measured UV index. Figure 6 shows that UV Index values of 8 (classified as 'very high') or greater were attained episodically from late October to early November. These events coincided with the site being under the ozone hole. During mid-November, the ozone hole broke down (metric 8 of Table 1), which was likely responsible for the UV Index remaining below 8 for the remainder of the year.

Figure 6 Total column ozone in Dobson units (— left axis) obtained from version 8.5 OMI overpass data and daily UV Index (— right axis) during 2013 for Davis, Antarctica. The 220 DU ozone hole threshold is also marked (— left axis).

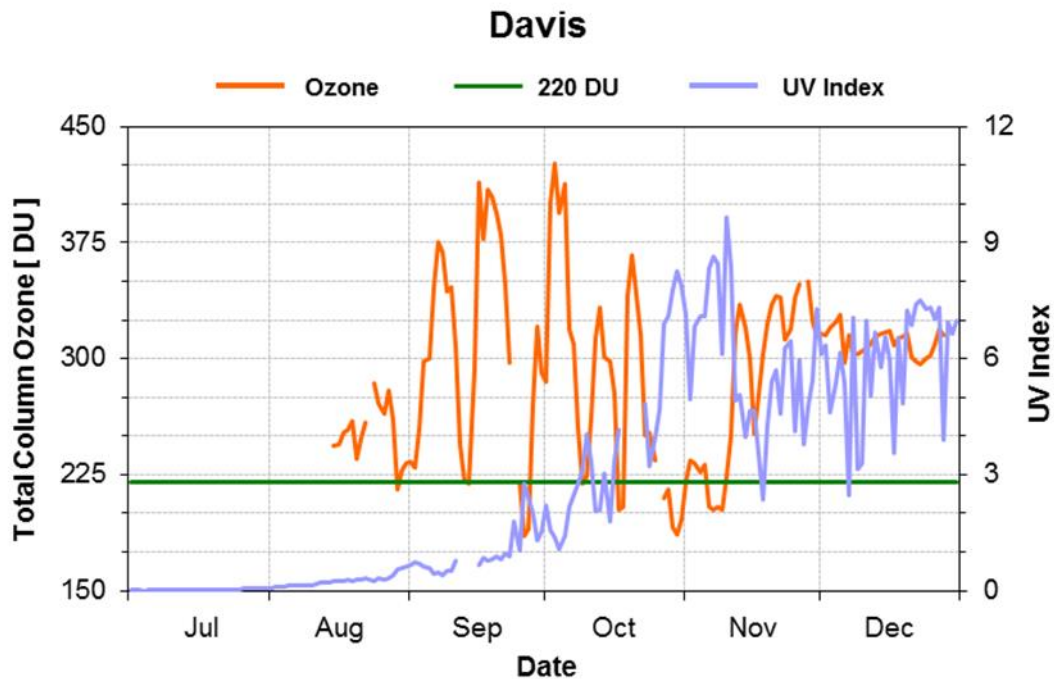


Figure 7 summarises the number of days between September and December that the UV Index attained 8 or greater at Casey, Davis and Mawson from 2007 to 2013. Casey receives less exposure to the highest UV Index values than the other sites, and Mawson appears to have slightly higher exposure than Davis. Casey is the furthest north of the sites, while Davis is the furthest south suggesting a simple relationship with the latitude of the stations does not explain the differences. The different responses across the sites may relate to local meteorological factors, but potentially also to the general climatological asymmetry in the shape of the ozone hole which tends to be displaced more poleward towards eastern longitudes. Also apparent in Figure 7 is that the number of days of very high and above levels in 2013 was relatively low compared with earlier years, but overall greater than for 2012.

## Conclusions

We have examined ozone concentrations and meteorological conditions in the Antarctic atmosphere during 2013 using a variety of data sources, including satellite remote sensing measurements, ground-based instruments and ozonesondes, and meteorological assimilations.

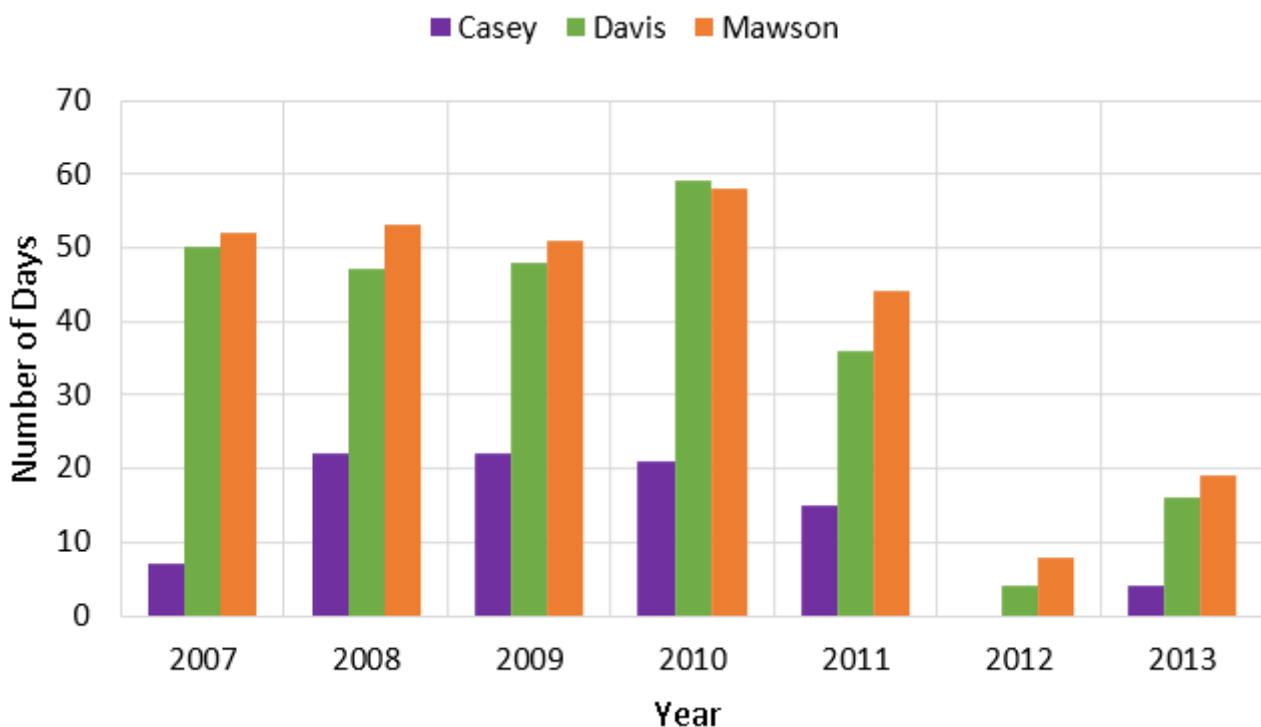
In terms of area, the Antarctic ozone hole in 2013 was the 17<sup>th</sup> largest on record (spanning the years 1979–2013, excluding 1995), attaining 24.0 million km<sup>2</sup> in mid-September. This was not an exceptionally notable value for this metric, but amongst the smallest since 1992 (excepting 2002, 2004, 2010 and 2012). At 1037 Mt, the total annual ozone deficit produced by the ozone hole of 2013 was the 19<sup>th</sup> largest on record and 41% of the peak value observed in 2006.

Despite the relatively modest ranking of the 2013 ozone hole in terms of overall severity, temperatures in the Antarctic lower stratosphere during winter were well below average, and at or near decadal lows. Anomalously cold lower stratospheric temperatures and dynamical indicators associated with the QBO and SAM indices, poleward heat flux and vortex area were all consistent with the polar vortex being in a relatively stable and strong configuration during winter, which would be expected to favour strong ozone loss in spring. Indeed, the ozone hole grew rapidly in August and at a rate similar to recent years of large ozone depletion. In common with years since the early to mid-1990s, SH stratospheric aerosol

levels in 2013 were near background levels (NASA, 2015), indicating that heterogeneous reactions during the Antarctic winter do not appear to have been unusually influenced by volcanic aerosols.

Despite the relatively rapid development of the 2013 ozone hole, dynamical disturbance and anomalous warming of the polar vortex began in late August. The level and persistence of the disturbances was likely an important factor in limiting the overall severity of ozone loss for the year, and causing the ozone hole to dissipate relatively early compared with most other years on record. The overall decline in the metrics of the ozone hole from late-September, and the relatively early breakdown date (mid-November) showed characteristics similar to those observed in 2012 when disturbances to the polar vortex during spring were also particularly pronounced.

Figure 7 Number of days between 1 September and 31 December each year between 2007 and 2013 that the UV index, as measured at Casey, Davis and Mawson (Antarctica) was 8 (very high) or greater. No measurements were made at Mawson in December 2007.



## Acknowledgements

We acknowledge the Department of Environment for support of this work, and the assistance of the following people: Jeff Ayton and the Australian Antarctic Division's Antarctic Medical Practitioners in collecting the solar UV data, BoM observers for collecting upper air measurements, and for expeditioners of the British Antarctic Survey for collecting the Halley measurements. Odin is currently a third-party mission for the European Space Agency. OSIRIS operations and data retrievals are primarily supported by the Canadian Space Agency. The OMI ozone data are courtesy of the Ozone Processing Team at NASA Goddard Space Flight Center. Aura/MLS data used in this study were acquired as part of the NASA's Earth-Sun System Division and archived and distributed by the Goddard Earth Sciences (GES) Data and Information Services Center (DISC) Distributed Active Archive Center (DAAC). UKMO data were obtained from the British Atmospheric Data Centre (<http://badc.nerc.ac.uk>). NCEP-DOE Reanalysis 2 data provided by the NOAA/OAR/ESRL PSD, Boulder, Colorado, USA, from their Web site at <http://www.esrl.noaa.gov/psd/>. Part of this work was performed under Project 4012 of the Australian Antarctic Science programme.

## References

Baldwin, M. P. and Dunkerton, T.J. 1998. Quasi-biennial modulations of the Southern Hemisphere stratospheric polar vortex. *Geophys. Res. Lett.*, 25, 3343-3346.

- Baldwin, M.P. and Dunkerton, T.J. 2001. Stratospheric harbingers of anomalous weather regimes. *Science*, 294, 581-4.
- BAS (British Antarctic Survey) 2014. Provisional Monthly Mean Ozone Values for Halley [online]. Available: <http://www.antarctica.ac.uk/met/jds/ozone/data/ZOZ5699.DAT> [Accessed 31 March 2015].
- Blunden, J. and D. S. Arndt, Eds., 2014: State of the Climate in 2013. *Bull. Amer. Meteor. Soc.*, 95, S1–S279. doi: <http://dx.doi.org/10.1175/2014BAMSStateoftheClimate.1>
- Dameris, M. and Godin-Beekmann, S. (Lead Authors), Alexander, S., Braesicke, P., M. Chipperfield, M., de Laat, A.T.J., Orsolini, Y., Rex, M. and Santee, M.L. 2014, Update on Polar ozone: Past, present, and future, Chapter 3 in *Scientific Assessment of Ozone Depletion: 2014*, Global Ozone Research and Monitoring Project – Report No. 55, World Meteorological Organization, Geneva, Switzerland.
- Fortuin, J.P.F. and Kelder, H. 1998. An ozone climatology based on ozonesonde and satellite measurements, *J. Geophys. Res.* 103, 31709-31734.
- Fraser, P., Krummel, P., Steele, P., Trudinger, C., Etheridge, D., Derek, D., O'Doherty, S., Simmonds, P., Miller, B., Muhle, J., Weiss, R., Oram, D., Prinn, R. and Wang R. 2014, Equivalent effective stratospheric chlorine from Cape Grim Air Archive, Antarctic firn and AGAGE global measurements of ozone depleting substances, *Baseline Atmospheric Program (Australia) 2009-2010*, Derek, N., Krummel, P. and Cleland, S. (eds.), Australian Bureau of Meteorology and CSIRO Marine and Atmospheric Research, Melbourne, Australia, 17-23.
- Kanamitsu, M., Ebisuzaki, W., Woollen, J., Yang, S.-K., Hnilo, J.J., Fiorino, M. and Potter, G.L. 2002. NCEP-DEO AMIP-II Reanalysis (R-2). *Bulletin of the American Meteorological Society*, 83, 1631–1643.
- Klekociuk, A.R., Tully, M.B., Alexander, S.P., Dargaville, R.J., Deschamps, L.L., Fraser, P.J., Gies, H.P., Henderson, S.I., Javorniczky, J., Krummel, P.B., Petelina, S.V., Shanklin, J.D., Siddaway, J.M. and Stone, K.A. 2011. The Antarctic Ozone Hole during 2010. *Aust. Met. Oceanogr. J.*, 61, 253-267.
- Klekociuk, A.R., Tully, M.B., Krummel, P.B., Gies, H.P., Petelina, S.V., Alexander, S.P., Deschamps, L.L., Fraser, P.J., Henderson, S.I., Javorniczky, J., Shanklin, J.D., Siddaway, J.M. and Stone, K.A. 2014a. The Antarctic Ozone Hole during 2011. *Aust. Met. Oceanogr. J.*, 64, 293-311.
- Klekociuk, A.R., Tully, M.B., Krummel, P.B., Gies, H.P., Alexander, S.P., Fraser, P.J., Henderson, S.I., Javorniczky, J., Petelina, S.V., Shanklin, J.D., Schofield, R. and Stone, K.A. 2014b. The Antarctic Ozone Hole during 2012. *Aust. Met. Oceanogr. J.*, 64, 313-330.
- Knight, J.R., Austin, J., Grainger, R.G. and Lambert, A. 1998. A three-dimensional model simulation of the impact of the Mt. Pinatubo aerosol on the Antarctic ozone hole, *Q.J. R. Meteorol. Soc.*, 124, 1527-1558.
- Marshall, G. J. 2003. Trends in the Southern Annular Mode from observations and reanalyses. *J. Clim.*, 16, 4134-4143.
- NASA (National Aeronautics and Space Administration) 2015. Stratospheric Aerosol Optical Thickness [online], Goddard Institute for Space Studies. Available: <http://data.giss.nasa.gov/modelforce/strataer> [Accessed 31 March 2015].
- Schwartz, M. J., Lambert, A., Manney, G.L., Read, W.G., Livesey, N.J., Froidevaux, L., Ao, C.O., Bernath, P.F., Boone, C.D., Cofield, R.E., Daffer, W.H., Drouin, B.J., Fetzer, E.J., Fuller, R.A., Jarnot, R.F., Jiang, J.H., Jiang, Y.B., Knosp, B.W., Krüger, K.R., F. Li, J.-L. Mlynarczyk, M.G., Pawson, S., Russell III, J.M., Santee, M.L., Snyder, W.V., Stek, P.C., Thurstans, R.P., Tompkins, A.M., Wagner, P.A., Walker, K.A., Waters, J.W., and Wu, D.L. 2008. Validation of the Aura Microwave Limb Sounder temperature and geopotential height measurements, *J. Geophys. Res.*, 113, D15S11, doi: 10.1029/2007JD008783.
- Swinbank, R., and O'Neill, A.A. 1994. Stratosphere-troposphere data assimilation system. *Monthly Weather Review*, 122, 686-702.
- Tully, M.B., Klekociuk, A.R., Deschamps, L.L., Henderson, S.I., Krummel, P.B., Fraser, P.J., Shanklin, J.D., Downey, A.H., Gies, H.P. and Javorniczky, J. 2008. The 2007 Antarctic Ozone Hole. *Aust. Met. Mag.*, 57, 279–98.
- Tully, M.B., Klekociuk, A.R., Alexander, S.P., Dargaville, R.J., Deschamps, L.L., Fraser, P.J., Gies, H.P., Henderson, S.I., Javorniczky, J., Krummel, P.B., Petelina, S.V., Shanklin, J.D., Siddaway, J.M. and Stone, K.A. 2011. The Antarctic Ozone Hole during 2008 and 2009. *Aust. Met. Oceanogr. J.*, 61, 77-90.
- Watson, P.A.G. and Gray, L.G. 2014. How does the Quasi-Biennial Oscillation affect the stratospheric polar vortex? *J. Atmos. Sci.*, 71, 391–409. doi: <http://dx.doi.org/10.1175/JAS-D-13-096.1>
- WHO (World Health Organization) 2002. *Global Solar UV Index: A Practical Guide*, ISBN 2 4 159007 6, Geneva.

## Appendix

### Polar temperatures and atmospheric indices

Monthly mean temperatures in the lower stratosphere above Antarctica during 2013 were below normal from January to August, and were markedly warm from mid-spring to early summer, particularly at pressures of 50 hPa and higher. Figure 8a shows monthly temperature anomalies for the latitude range 90°S to 65°S from the National Centers for Environmental Prediction (NCEP) – Department of Energy (DOE) Reanalysis 2 data (Kanamitsu et al., 2002) with respect to the base period 1979–2012 for three pressure levels. Temperatures at 10 hPa were consistently below the climatological mean from January to August and again in November and December. At the 50 hPa and 100 hPa levels, temperatures from May to August were at or near the lowest levels for the preceding decade. At these levels from September to November, 2013 was ranked amongst the three warmest years in the preceding decade, although temperatures in these months were generally not as extreme as in 2012 (Klekociuk et al., 2014b). Temperatures in December at 100 hPa were also anomalously warm.

During 2013, the NCEP standardised 30 hPa Quasi-Biennial Oscillation (QBO) index (URL <http://www.cpc.ncep.noaa.gov/data/indices/qbo.u30.index>) was switched from negative (westward) from March to be consistently positive (eastward; Figure 8b, top panel). The QBO modulates the ability of upward propagating planetary waves to influence extratropical latitudes in the winter hemisphere. A stronger and less disturbed polar vortex is preferentially observed during the positive QBO index or phase (Baldwin and Dunkerton, 1998; Watson and Gray, 2014).

The surface standardised Southern Annular Mode (SAM) index (Marshall, 2003 and URL <http://www.antarctica.ac.uk/met/gjma/sam.html>) (Figure 8b, middle panel) was mostly positive during the year. The surface SAM index was negative in April and again from August to October; the August value was notable in being the most negative value for all years since 1979. As discussed in Baldwin and Dunkerton (2001), positive (negative) anomalies in the stratospheric SAM tend to occur preferentially under conditions of a strong (weak) polar vortex (corresponding to positive (negative) QBO phase) – these conditions are generally confined to the winter and spring seasons in the Southern Hemisphere when the polar vortex exists. Stratospheric and tropospheric SAM variations are sometimes independent, but as noted in Baldwin and Dunkerton (2001), SAM anomalies in the lowermost stratosphere tend to favour tropospheric SAM anomalies of the same sign. The bottom panel of Figure 8b shows the SAM index for 50 hPa evaluated using empirical orthogonal function analysis of NCEP Reanalysis-2 data, following the approach used by the NOAA Climate Prediction Center for their 700 hPa Antarctic Oscillation index (URL [http://www.cpc.ncep.noaa.gov/products/precip/CWlink/daily\\_ao\\_index/ao/ao\\_index.html](http://www.cpc.ncep.noaa.gov/products/precip/CWlink/daily_ao_index/ao/ao_index.html)). The 50 hPa SAM index was generally weak in 2013, except from August through December when it was strongly negative. Importantly, the surface and stratospheric SAM indices from August to October were both negative, which would expect to favour weakening and disturbance to the vortex, and this was potentially a factor responsible for the warm temperature anomalies at the 50 and 100 hPa levels from September to November.

Daily temperature anomalies averaged over the Antarctic region obtained from measurements by the Microwave Limb Sounder (MLS) on the Aura spacecraft (Schwartz et al., 2008) are shown in Figure 9. A marked feature in this figure is the band of anomalously warm temperatures that appears near the stratopause from May and which moved progressively down to reach the tropopause region (near 10 km altitude) by the end of the year. Significant cold anomalies are apparent from July to August between 15 and 25 km.

### Dynamical activity

The poleward transport of heat provides a useful indicator of dynamical disturbances to the polar atmosphere produced by planetary waves at low- and mid-latitudes. Figure 10 shows the evolution of heat flux (measured by the product of the zonal anomalies in temperature and meridional wind speed) during 2013 using assimilated meteorological data from the United Kingdom Meteorological Office (UKMO). Outbreaks of poleward heat transport in the mid- and upper stratosphere (pressure levels 10–0.2 hPa) occurred from May through to mid-October at mid-latitudes (top panel of Figure 10). At higher latitudes, heat transport was only able to penetrate from late July to late October. The most significant episode of poleward heat transport occurred in mid-September and this coincided with the off-pole displacement of the vortex that caused high ozone levels above Davis noted in the discussion relating to Figure 5.

### The Polar Vortex

Timeseries of proxies for the areal extent of the stratospheric polar vortex are shown in Figure 11 for the 450 K and 850 K isentropic surfaces. For the 450 K isentrope (Figure 11a), the vortex area was mainly close to the climatological mean up to mid-October, after which the area decreased abruptly to lie well below the mean for the remainder of the year. The progression of the vortex area at 850 K over the year (Figure 11b) was generally close to or slightly below the climatological mean (except for a period of above average size near the start of August).

Figure 8(a) Monthly temperature anomalies (K) from zonal means for the latitude range 65 °S to 90 °S from NCEP Reanalysis-2 data relative to the monthly climatology for 1979-2012 at pressure levels of 10 hPa (top), 50 hPa (middle) and 100 hPa (bottom). Coloured bars show monthly anomalies for 2013, and diamonds connected by solid lines show maximum and minimum anomalies for 1979-2013. Numbers at the top of each panel are the rank of 2013 relative to years 2004-2013 (1 [10] = most positive [most negative] anomaly), and numbers at the bottom of each panel are values (K) of the monthly anomalies for 2013. Values for 2012 are shown as black crosses.

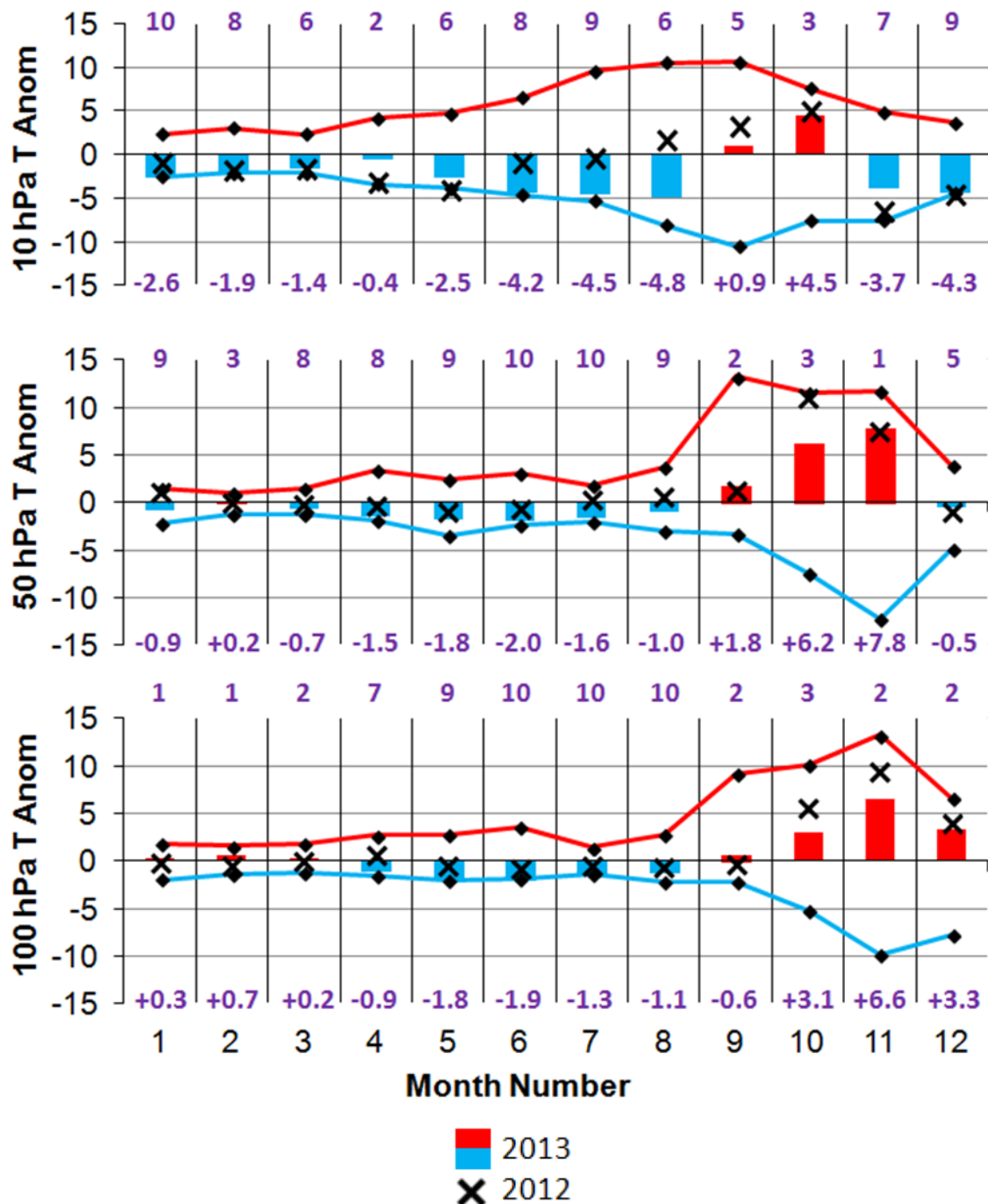


Figure 8(b) Monthly (top) NCEP standardised 30 hPa Quasi-Biennial Oscillation (QBO) index, (middle) standardised surface Southern Annular Mode (SAM) index (Marshall, 2003), and (bottom) standardised SAM index evaluated at 50 hPa (see text for details). The indices are expressed in standard deviations relative to base period of 1983-2012 (for QBO) and 1979-2000 (for SAM). Diamonds connected by solid lines show maximum and minimum anomalies for each index over the period 1979-2013. Values for 2012 are shown as black crosses.

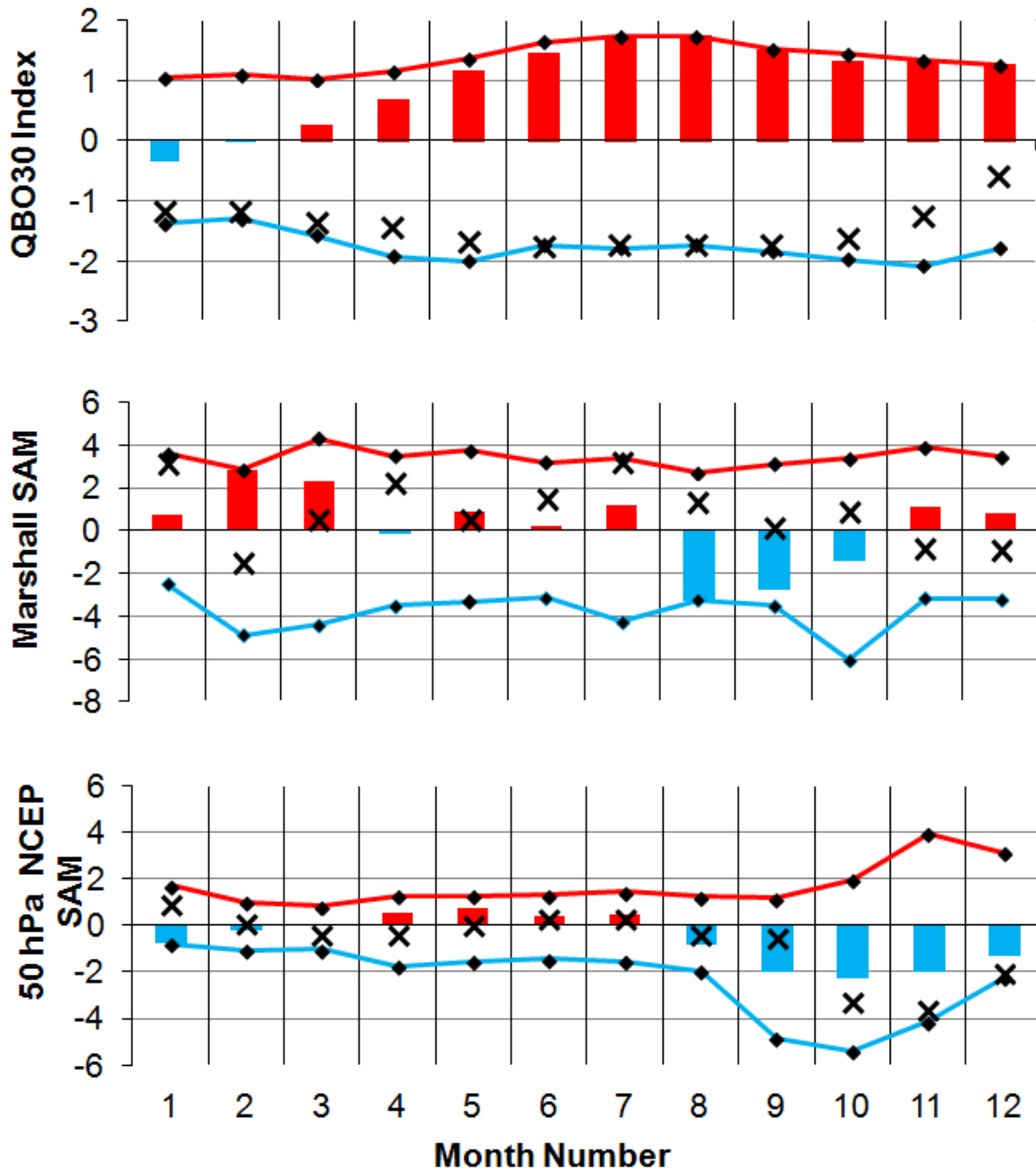


Figure 9 Daily time-height section of anomalies of the zonal average air temperature over latitudes  $65^{\circ}\text{S}$  to  $85^{\circ}\text{S}$  from Aura Microwave Limb Sounder (MLS) quality controlled version 3.3 data for 2013. The anomalies are evaluated relative to the base period of 8 August 2004 (the start of measurements) to 31 December 2012. The solid black line marks the height of the warm-point stratopause in 2013, while the white dashed line marks the average warm-point stratopause height over the climatological period. The white bar marks missing data. Single diagonal hatches marks anomalies that are outside the interdecile range based on measurements prior to 2013. Crossed diagonal hatching marks anomalies that are at the daily maximum or minimum value for all measurements up to and including those of 2013.

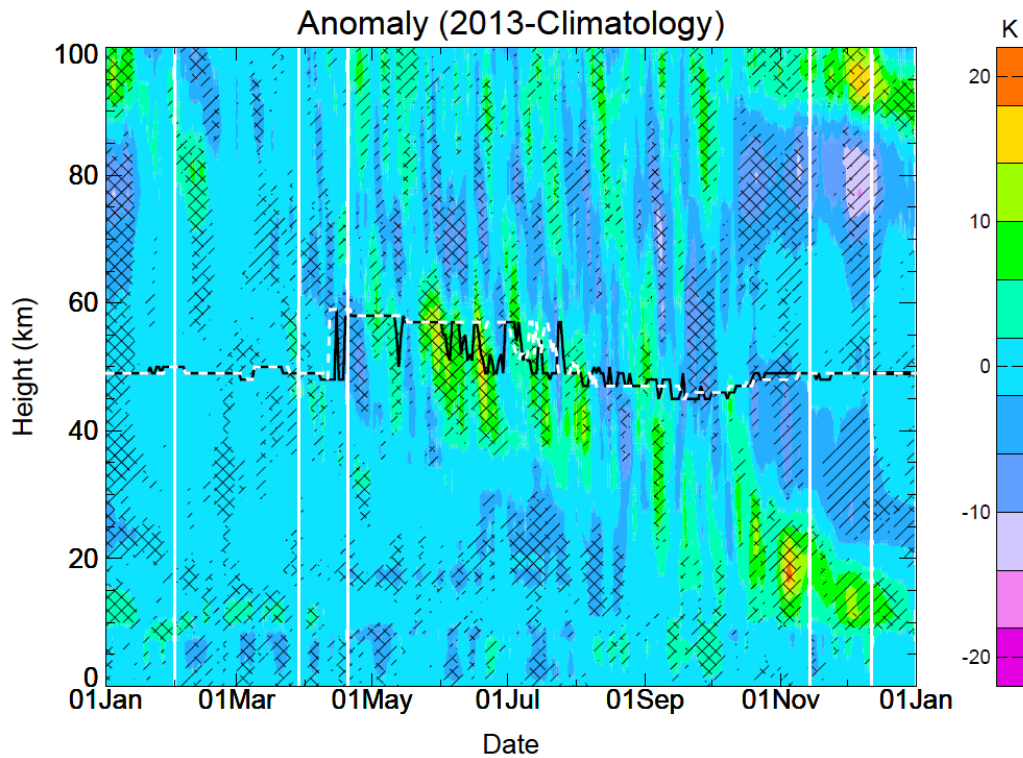


Figure 10 Daily eddy heat flux for 2013 averaged between latitudes of (a) 35 °S to 55 °S and (b) 65 °S and 85 °S as a function of pressure evaluated from UKMO Stratospheric Assimilated Data (Swinbank and O’Neill, 1994). Negative values indicate poleward transport of heat. The zero contour is outlined in white.

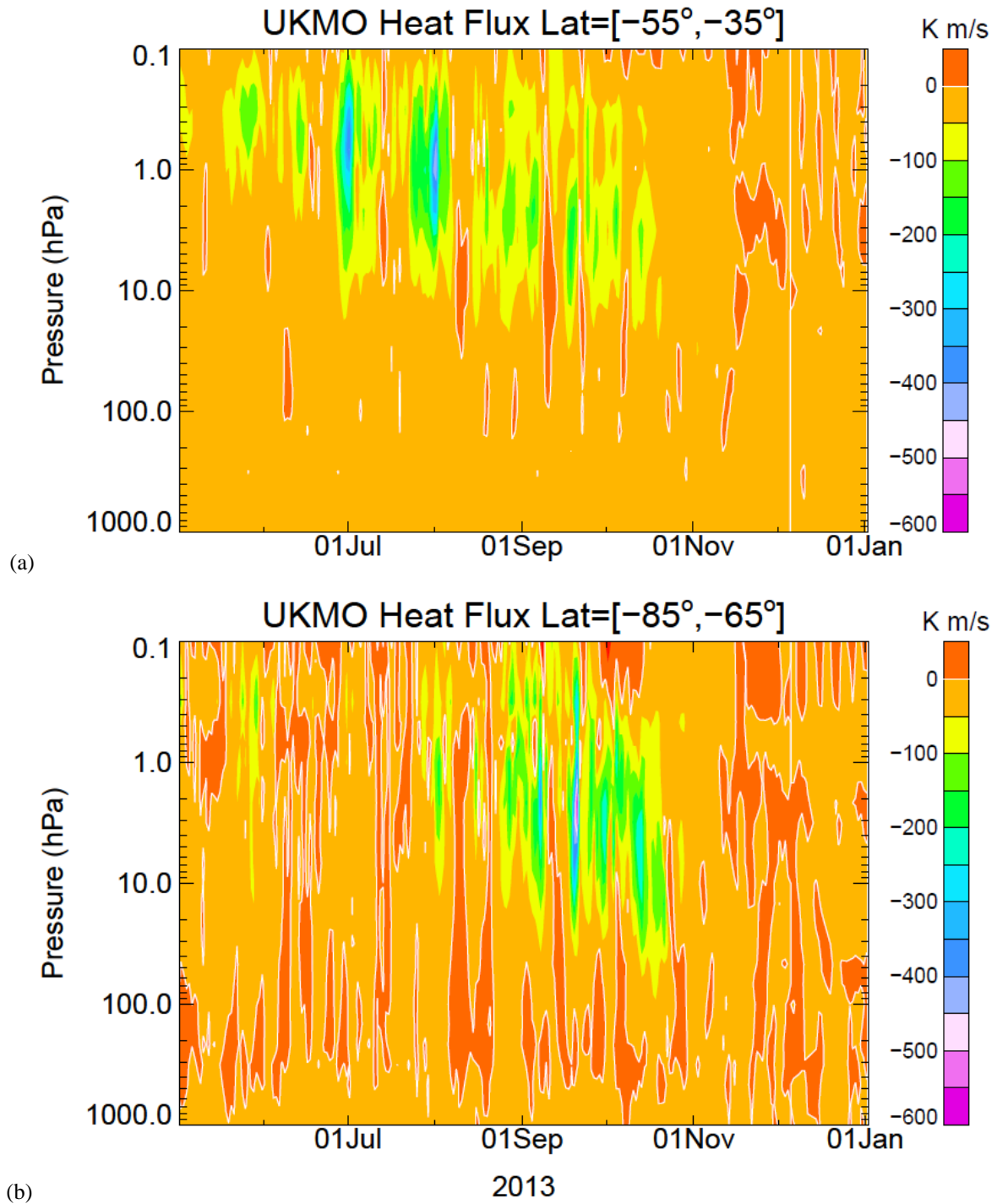


Figure 11 Southern Hemisphere vortex area evaluated on potential temperature ( $\theta$ ) surfaces of (a) 450 K (~18 km height) and (b) 850 K (~31 km height). The time-series for 2013 is shown in black; the blue time-series is the mean for 1992-2013, while the lower and upper red time-series in each graph show the 5th and 95th percentiles, respectively, for 1992-2013. The vortex area is evaluated using data from the UKMO stratospheric assimilation, and represents the surface area enclosed by potential vorticity contours of (a) -30 PVU and (b) -600 PVU.

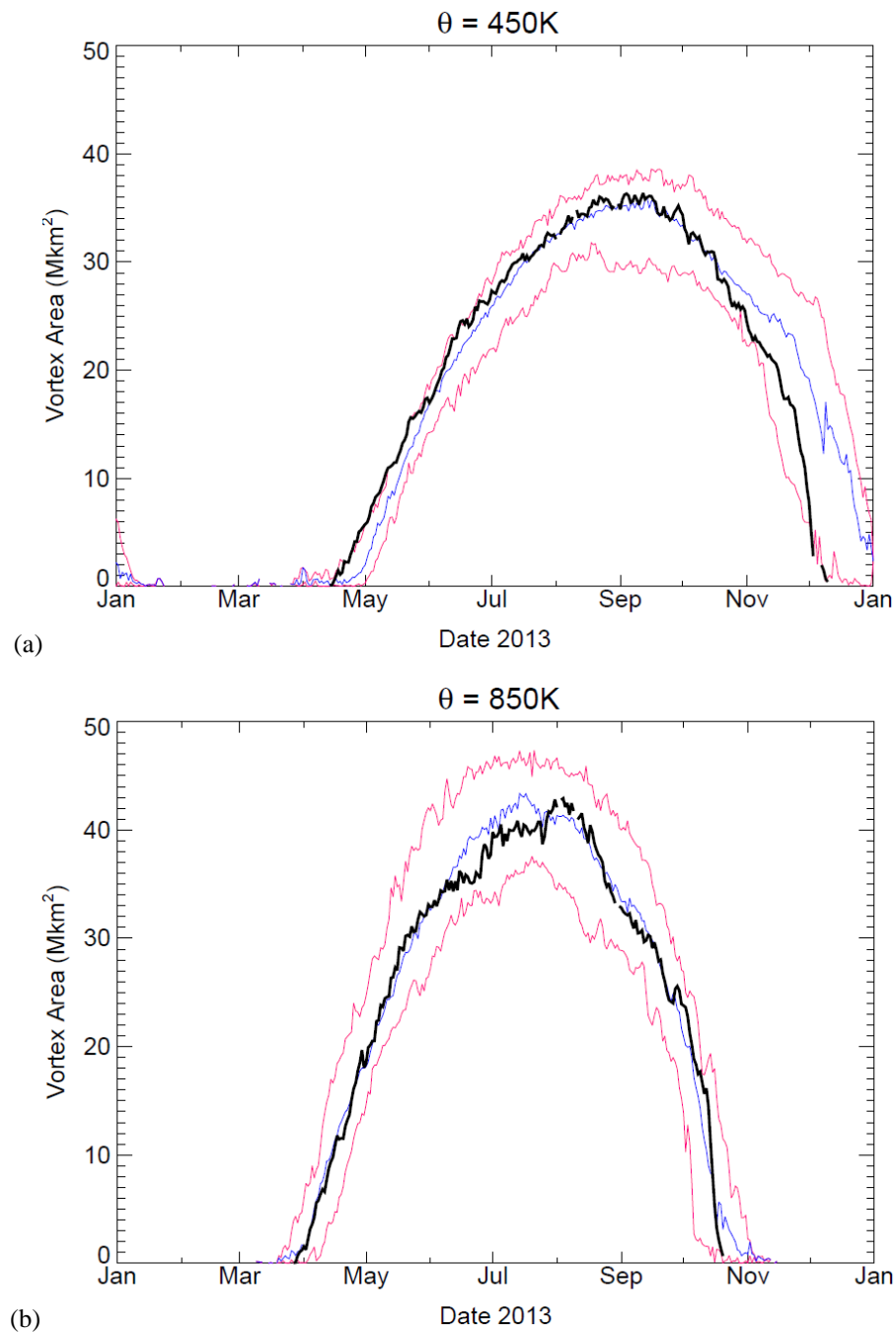
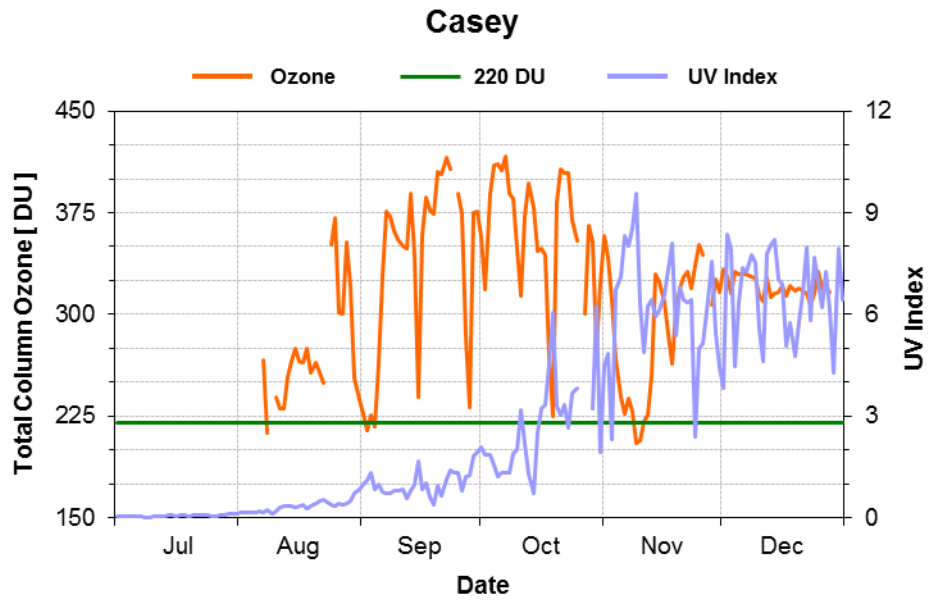
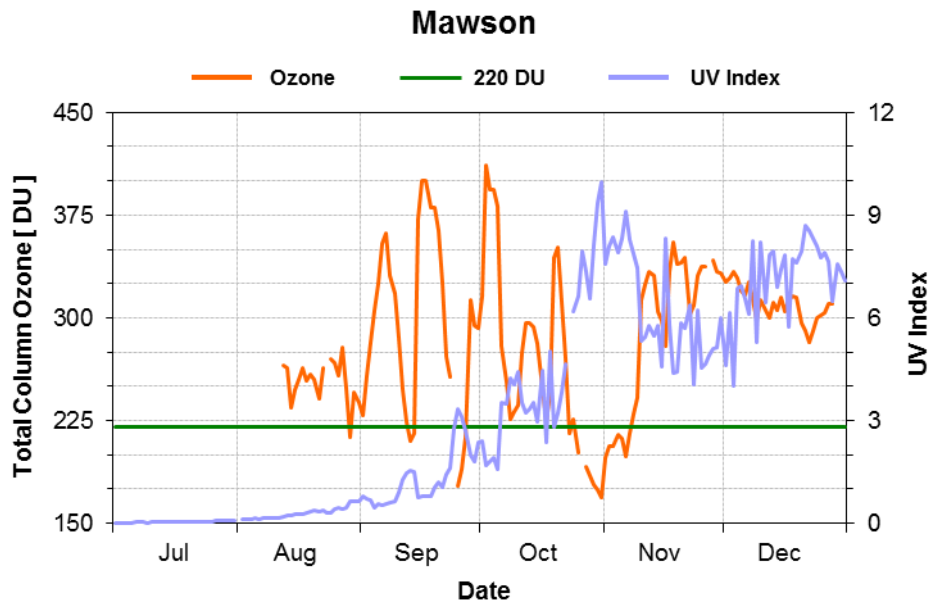


Figure 12 Total column ozone in Dobson units (— left axis) and daily UV Index (— right axis) during 2013 for (a) Casey (66.3 °S, 110.5 °E) and (b) Mawson (67.6 °S, 62.9 °E). The 220 DU ozone hole threshold is also marked (— left axis).



(a)



(b)